

A Visibility Matching Technique for Efficient Millimeter-wave Vehicular Channel Modeling

Sajjad Hussain* and Conor Brennan†

Abstract

Site specific propagation models for highly dynamic vehicle-to-vehicle scenarios become time consuming as the identification of visible surfaces must be performed independently for each transmitter location. Moreover the validation of higher order of ray interactions presents a significant computational overhead. This paper presents an efficient ray-tracing algorithm for vehicle-to-vehicle propagation prediction. The model presented in this paper extends a previous model that uses a pre-computed database of intra-visibility of walls and edges in the environment. The model computes the list of faces and edges that are directly visible to the mobile receiver. This visibility information is then used to reduce the image-tree thereby accelerating the ray validation. The paper also presents an efficient technique to compute diffuse scattered rays in a timely manner. The validation results show considerable time saving over previous models.

1 Introduction

Vehicular communication is characterized by high mobility within dynamic environments that poses a great limitation on accurate modelling of the radio channel. Accurate channel prediction requires that significant propagation mechanisms including reflections, diffraction and rough surface scattering from all the objects in the environment are properly modeled. A ray-tracing model considers all the scattering objects in the environment and computes the dominant paths, or rays, up to a specified order between the transmitter and receiver. The computationally intensive tasks in ray-tracing models for vehicular communications include the identification of visible surfaces for the mobile transmitter using the so-called visibility algorithms; and validation of diffuse scattering rays and specular rays of higher order. Since the visibility is constantly changing in highly dynamic vehicular scenarios, identification of visible scatterers requires significant pre-processing that makes the ray-tracing models less attractive for propagation modeling in vehicular networks [1]. However, recent works have proposed dynamic ray tracing to compute Doppler shifts [2] and tracking of ray interaction points [3] in highly dynamic vehicle-to-vehicle scenarios.

Many time efficient ray tracing models for *static transmitters* have been proposed in the literature. However, application of these models in moving transmitter scenarios requires that some pre-processing be performed at each transmitter location. This increases the overall simulation time to limit their application in moving transmitter scenarios. Previous work [4] by the authors proposed an efficient model to compute image-tree of required order of ray interaction along the path of a mobile transmitter. This paper extends the previous work by selecting a smaller subset of image-tree for each transmitter-receiver pair that can produce all the valid higher order rays in vehicular scenarios. Additionally, this paper incorporates previous work to efficiently compute the exact visible surfaces that contribute diffuse scattering for accurate radio channel modeling in vehicular networks. The precise location of visible scattering surfaces in the environment can aid in the design and performance evaluation of so-called smart radio environments based on re-configurable intelligent surfaces, which are being investigated for 5G and beyond networks. The

*National University of Sciences and Technology (NUST) Pakistan. email:sajjad.hussain2@seecs.edu.pk

†School of Electronic Engineering, Dublin City University, Ireland. email:conor.brennan@dcu.ie

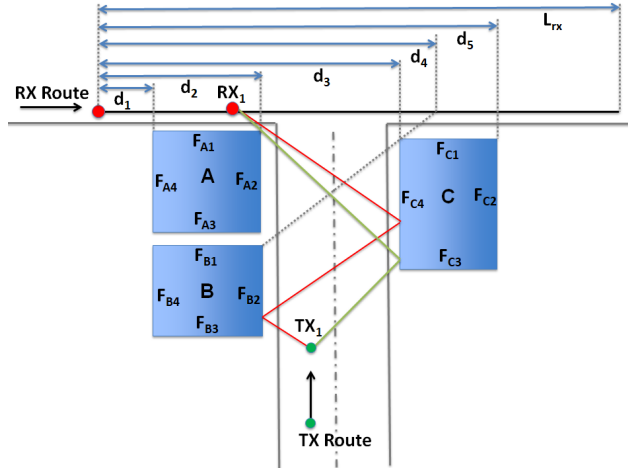


Figure 1: Computation of visibility table for the mobile receiver in a typical V2V scenario.

model proposed in this work considers a static environment although mobile scatterers can be included as in previous work [5]. Vegetation loss is also not included for simplicity but it can be incorporated into the results as a post-processing step, as shown in reference [6].

2 The Ray-Tracing Algorithm

2.1 Visibility Computations for Mobile Transmitter

A mobile transmitter in an outdoor environment interacts with a set of visible scatterers, the precise composition of which continually changes as it moves. The algorithm presented in [4] computes the so-called *visibility table* for required order of ray interaction for a mobile transmitter. This visibility table contains the list of all scatterers that are visible to the mobile transmitter for its entire length of motion along with the distance (from a reference point) for which these scatterers remain visible. Further details to compute the image-tree of required order of ray interaction for the mobile transmitter can be found in [4].

2.2 Visibility Computations for Mobile Receiver

The image-tree for a mobile transmitter at each location along its route is readily available from the visibility table. When computing propagation to a given receiver location a ray-tracing model uses a recursive algorithm to perform ray validation test for each image in the image-tree. This validation test may become time consuming if the image-tree size is considerably large or a higher order of ray interaction is computed. It has been observed that only a certain fraction of the image-tree produce valid rays and therefore large computational resources are wasted in geometrical checks. This paper presents a solution to check only a subset of the image-tree that may produce the valid rays. In order to achieve this, we make use of the fact that a receiver location can receive a valid ray whose final segment emanates only from the scatterers (building walls for example) that are *directly visible* to it. Therefore, the list of all the faces and edges that are directly visible to the receiver must be computed. Since the receiver is constantly moving in a V2V scenario, a pre-processing step is included to determine the first order visibility table for the moving receiver. i.e. the list of all the faces and edges that are visible to the receiver along with the distance for which these remain visible is computed in this step. Consider a typical V2V scenario at an urban street intersection in Fig. 1. Only three buildings *A*, *B* and *C* are considered in the environment for simplicity. The distances from the start point of the receiver for which the different faces remain visible, either partially or completely to the receiver are shown. It can be seen that faces

Table 1: Visibility table for the receiver considered in the example environment shown in Fig. 1

Visible Node	Visibility Range	
	d_i	d_f
F_{A1}	0	L_{rx}
F_{C1}	0	L_{rx}
F_{A4}	0	d_1
F_{B4}	0	d_1
F_{C4}	0	d_3
F_{A2}	d_2	L_{rx}
F_{B2}	d_2	d_4
F_{C2}	d_5	L_{rx}

F_{A4} and F_{B4} remain visible to receiver up to distance d_1 . Face F_{C4} remains visible up to distance d_3 . Face F_{B2} remains visible when receiver is between the distance d_2 and d_4 . Face F_{A2} remains visible from d_2 to the final position of the receiver at distance L_{rx} . Faces F_{A1} and F_{C1} both remain visible for the entire length of receiver route. Face F_{C2} remains visible for a short distance between d_5 and L_{rx} . This visibility information is summarized in the visibility table shown in Table 1. The visibility range of each face is specified by the distance from start position of the receiver at which it starts becoming visible (d_i) and the distance up to which it remains visible (d_f) to the receiver in Table 1.

2.3 Visibility Matching for Image Tree Reduction in V2V scenarios

The algorithm proposed in previous work (section-II E of [4]) readily produces the image-tree, i.e. the list of all the visible faces and edges of required order of ray interaction for the mobile transmitter. The visibility table for the mobile receiver, as discussed in the above section, gives a list of all the faces and edges that are directly visible. The speed of the mobile receiver is assumed to be known so that its distance from the start point can be computed at any given time instance. This distance information is used to extract the list of faces and edges from the receiver’s visibility table that are visible to the receiver at that time instance. In order to compute the reduced image-tree, the nodes in the transmitter’s image-tree are compared with the list of faces and edges visible to the receiver as given by the receiver’s visibility table at each time instance. This so-called *visibility matching* is performed one-on-one to check if the entries in both the lists are associated with the same face or edge of a building. All the nodes in the transmitter’s image-tree that match with the entries in receiver’s visibility list are grouped to form a subset of the image-tree that may produce the valid rays. An image-tree has multiple layers corresponding to the order of the ray-interaction to be computed. Therefore if a node located at second or higher layer of the transmitter’s image-tree is matched with a node in the receiver’s visibility list, it is included in the reduced subset of the image-tree along with its parent images. This can be further explained with the help of Fig. 1. The mobile transmitter at TX_1 is located such that faces F_{B3} , F_{C3} , F_{A2} , F_{B2} , and F_{C4} are directly visible to it and form the first order images of the image-tree. Furthermore, F_{C3} and F_{C4} are visible to F_{B2} ; and F_{A2} is visible to F_{C4} for the given transmitter location. These faces are used to form the second order images in the image-tree which is shown on the left side in Fig. 2. The receiver RX_1 is located between the distance d_1 and d_2 from the start point so that only faces F_{A1} , F_{C1} and F_{C4} are visible to it as per data previously gathered in the visibility table. The receiver may receive valid rays only from these three faces. If the visibility list for the receiver is matched with the image-tree, it is evident that only the face F_{C4} is a viable common node that can produce valid rays at the receiver. It is directly visible to the receiver as well as included as a first order and a second order image in the image-tree. The image-tree can thus be reduced to the form shown on the right side of Fig.2. This simple example shows that an

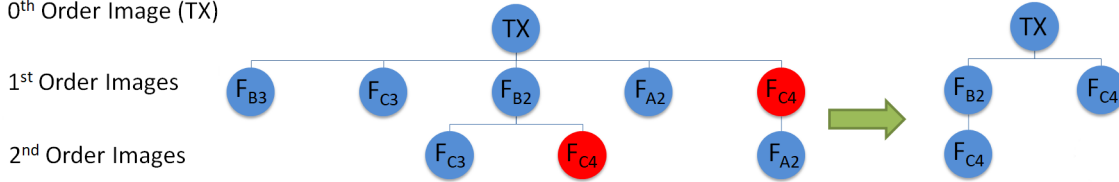


Figure 2: Reduction of image-tree using visibility matching

image-tree with nine nodes has been reduced to an image-tree with only four nodes. Geometrical checks can be performed to validate that only two rays exist between transmitter and receiver at this particular time instant as shown in Fig.1. The steps discussed above for ray-tracing can be summarized in the following algorithm.

Algorithm 1 Ray-tracing algorithm for vehicle-to-vehicle communications using visibility matching.

```

Compute visibility table of  $n^{th}$  order for transmitter [4];
Compute visibility table for receiver;
for  $i = 1$  to total_time_samples do
  Compute  $n^{th}$  order image-tree at  $t_i$  from visibility table for transmitter [4];
  Compute list of nodes directly visible to receiver at  $t_i$  from visibility table for receiver;
  for  $j = 1$  to total_nodes_visible_to_receiver do
    for  $k = 1$  to total_images_in_image_tree do
      if  $j^{th}$  node in visibility list of receiver matches with  $k^{th}$  node in image-tree then
        Add  $k^{th}$  image to the reduced image-tree;
      end if
    end for
  end for
  for  $p = 1$  to total_images_in_reduced_image_tree do
    Perform ray validation test for  $p^{th}$  image;
    if valid ray is found then
      Update rays database;
    end if
  end for
end for
Post-process rays database;

```

2.4 Computation of Diffuse scattering

Diffuse scattering from building facades becomes significant at and above sub-6 GHz band and must be incorporated into propagation models for accurate channel predictions [7]. It has been shown that inclusion of suitable order of ray interaction and use of a physically consistent effective roughness model to include diffuse scattering from building walls increases the accuracy of ray tracing models [8]. The section of the faces of buildings that are commonly visible to both the transmitter and receiver produce first order diffuse scattering. The visible section of the face is divided into a grid of rectangular tiles and scattering contribution from each tile is computed [8]. The geometrical checks to validate the ray-segments (i.e. ensure visibility) from transmitter and receiver to each position on the grid of points on building faces must be performed efficiently. A better approach would be to use the so-called space-division technique in which a coarse grid is overlaid on the geographic area and the buildings contained within each grid-square are pre-computed. Firstly, a list of all the grid-squares that are intersected by the ray-segments from

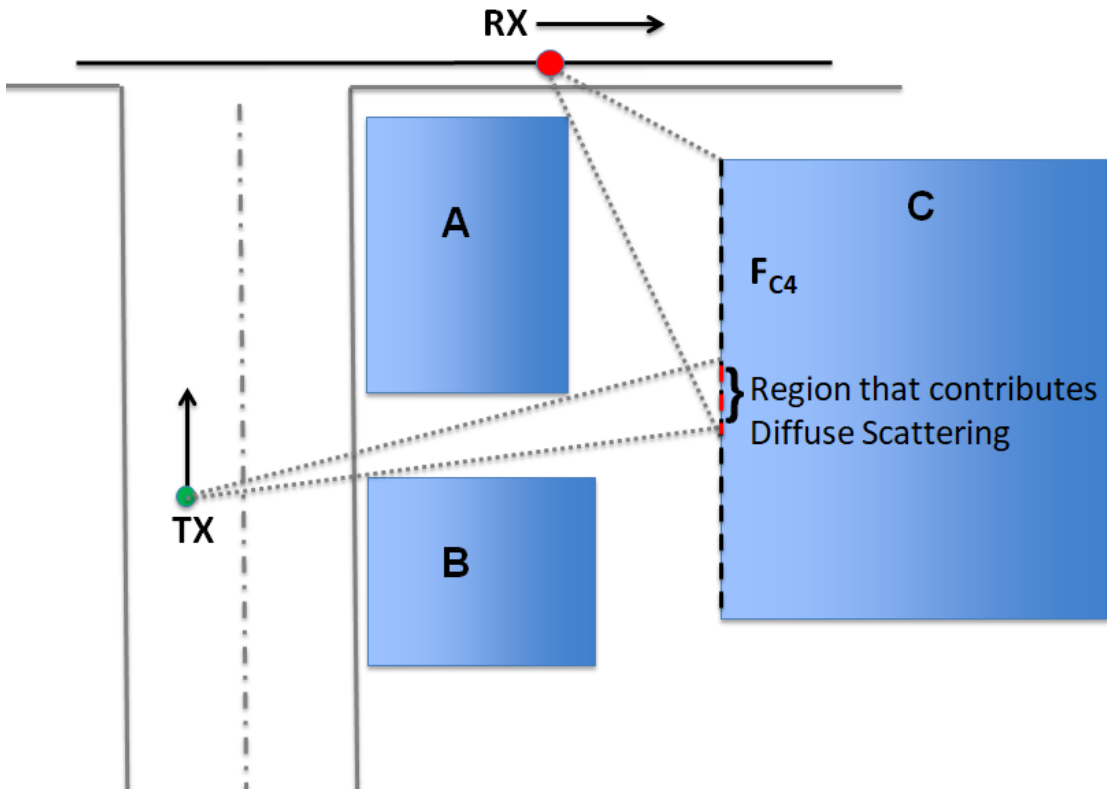


Figure 3: Computation of illuminated region of a face visible to a mobile receiver in horizontal plane for diffuse scattering.

transmitter and receiver to the interaction point on wall is computed. Then, only the buildings contained within the intersected grid-squares are checked for intersection with the ray-segments. Therefore, a speed-up in ray validation is achieved as only a limited number of buildings need be checked. Recent work by Dreyer et al. [9] proposed an efficient technique to compute diffuse scattering rays using the so-called location view database (LVD) obtained from the pre-computed surfaces visibility information. The mutually visible faces are referred to as *illuminated faces* in the discussion that follows. This section explains how we can use the visibility matching as discussed in section (2.3) and the intra-visibility matrix for efficient computation of diffuse scattering rays.

The illuminated faces are identified at each time instance by matching the *first order reflection images* in the transmitter's image-tree with the list of faces that are directly visible to the receiver as determined in the visibility table. However, we still need to determine the exact region of each illuminated face that is mutually visible to the transmitter and receiver and contributes diffuse scattering. In order to do this, first the mutually visible region in horizontal plane along the width of the building's face is determined. Each illuminated face is divided into a number of discrete segments spaced apart at small incremental distance in the horizontal plane between the vertical edges of the face along its width. A small incremental distance is used according to the required dimensions of tiles in the rectangular grid for computation of the diffuse scattering contribution. The results presented in this paper use a tile size of $5\text{cm} \times 5\text{cm}$ which corresponds to $1\lambda \times 1\lambda$ at 5.9 GHz . The discrete segments along the width of illuminated face are considered at the same height as that of the transmitter. Horizontal lines are drawn from the transmitter and receiver to the centre point of each discrete segment along the width of the illuminated face. These line from transmitter and receiver to the points on the illuminated face must be checked for obstruction by any other building in the environment. This paper uses *intra-visibility matrix* for ray-segments

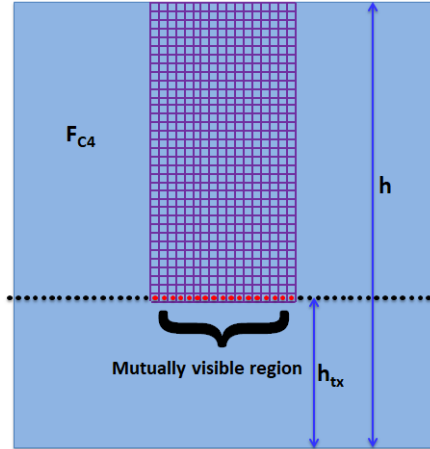


Figure 4: Computation of illuminated region of a face visible to a mobile receiver in vertical plane for diffuse scattering.

validation. The list of faces that are visible to the illuminated face is readily available from the intra-visibility matrix. Instead of checking all or a subset of all the buildings' faces, only the list of faces that are visible to the illuminated face, as available from the intra-visibility matrix, are checked for obstruction. The line of consecutive discrete points on the illuminated face for which the ray-segments are not obstructed by any building in the environment produces the width of the face that is mutually visible to the transmitter and receiver. This mutually visible horizontal section along the width of illuminated face is then extended vertically up to the height of the face to obtain a grid of tiles that contributes diffuse scattering. This is based on the assumption that there are no other vehicles taller than the transmitter vehicle and the mutually visible horizontal section on the illuminated face remains entirely visible to both the transmitter and receiver above the height of the transmitter antenna. The rays below the height of the transmitter antenna are assumed to be blocked due to other vehicles and are therefore left out in this model.

The technique proposed in this paper achieves speed-up in the computation of diffuse scattering rays in two ways. Firstly, the visibility table for the receiver readily produces the potential building faces that may contribute diffuse scattering. By matching these faces with the list of first order reflection images produces the list of illuminated faces at each time instance. Secondly, this paper uses intra-visibility matrix to validate the horizontal ray-segments from transmitter and receiver to the discrete points on illuminated face for determination of mutually visible region. This is further explained with the help of Figures 3 and 4. Face F_{C4} is visible to both the transmitter and receiver. Horizontal discretization is performed along the width of the face at transmitter height h_{tx} as shown. The width of face F_{C4} marked in red shows the region that is mutually visible to transmitter and receiver. This is the required horizontal section of the face that contributes diffuse scattering at the receiver. After the mutually visible region along the width of illuminated face is found, a grid of tiles from these points up to the height of F_{C4} (h) is computed as shown in Fig. 4.

3 Results

The algorithms described in this paper were used to simulate vehicle-to-vehicle communication scenarios at an urban street intersection. The simulated environment, taken from Munich city [10], consists of 67 buildings and is shown in Fig. 5. The transmitter vehicle is moving towards the street intersection and the same transmitter route is considered for both a line of sight (LOS) and a non line of sight (NLOS) configuration. Transmitter and receiver vehicles are moving at the speed of 10 m/s. The heights of both the transmitter and receiver antenna is assumed to be 1.6 m.

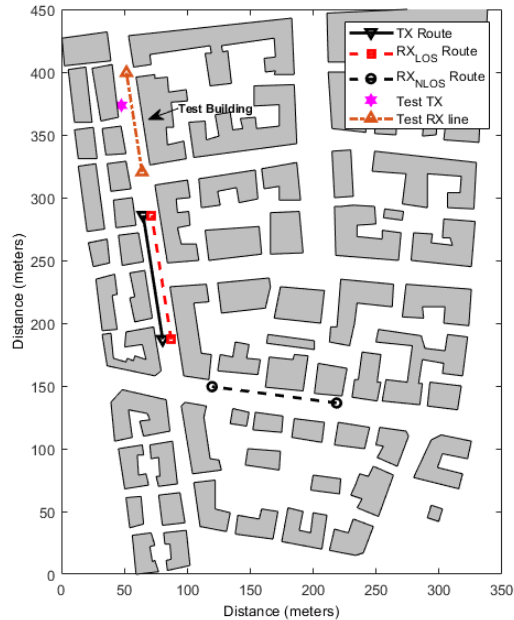


Figure 5: Geometry of simulated environment and mobile routes for LOS and NLOS scenarios.

The channel is simulated at 10ms resolution for a total time of 10 seconds for both configurations. Therefore a total of 1,000 channel snapshots are computed for distinguished transmitter-receiver pairs using the proposed ray-tracing algorithm.

The channel metrics are not computed for the simulated environment as measured data is not available for comparison. However, to demonstrate the contribution of diffuse scattering, the electric field is computed for specular reflection and specular reflection with diffuse scattering from a wall in the simulated environment for a test transmitter location and a line of receiver points (see Fig. 5). Diffuse scattering is computed using a Lambertian and a directive model adopted from [8] and is shown in Fig. 6. A half-wave dipole antenna for transmitter with 10dBm output power and standard electromagnetic parameters for brick wall ($\epsilon_r = 5$, $\sigma = 0.01$) are used in the simulations. Please note that the accuracy of our model in computing pathloss against the measured data and in finding rays as compared against a standard ray tracing model has already been reported in previous works [4, 11]. The channel is computed for a specified order of specular reflections, vertical edge diffraction and diffuse scattering. The time reduction achieved using the proposed algorithm is compared against the previous model [4] that in turn has been developed by incorporating previous works of the authors. Please note that the proposed model does not achieve time acceleration by simplification or omission of rays. The model computes all the *valid rays* of required order of ray interaction between each transmitter-receiver pair using a smaller image-tree obtained through visibility matching technique.

Tables 2 and 3 compare the total ray validation time using the previous model against the proposed algorithm for up to 6th order of *wall reflections only* in LOS and NLOS configurations respectively. The computation of visibility table for the receiver route takes 828 seconds and 1,233 seconds for LOS and NLOS scenario respectively. For up to 4th order of wall reflections the image-tree size at each transmitter location is not that large so that the total time for ray validation using the proposed model is not reduced by the margin of time required for visibility table computation. Therefore no time reduction for up to 4th order of wall reflection is achieved as can be seen in the tables. For 5th and 6th order of wall reflections, the proposed model reduces the ray validation time by 34.54% and 47.29% respectively for LOS scenario and by 24.82% and 39.97% respectively for NLOS scenario.

Tables 4 and 5 present the same comparison for up to 4th order of wall reflections and vertical

Table 2: Ray-tracing time comparison for only wall reflections in LOS scenario.

Time	Order = 1	Order = 2	Order = 3	Order = 4	Order = 5	Order = 6
Total time using [4] (seconds)	605	744	1,136	2,287	5,376	12,413
Pre-process time for <i>RX</i> route (seconds)	828	828	828	828	828	828
Ray validation time (seconds)	583	649	822	1,333	2,691	5,715
Total time using this paper (seconds)	1,411	1,477	1,650	2,161	3,519	6,543
Reduction	-133.22%	-98.52%	-45.25%	5.51%	34.54%	47.29%

Table 3: Ray-tracing time comparison for only wall reflections in NLOS scenario.

Time	Order = 1	Order = 2	Order = 3	Order = 4	Order = 5	Order = 6
Total time using [4] (seconds)	625	745	1,134	2,377	5,422	12,387
Pre-process time for <i>RX</i> route (seconds)	1,233	1,233	1,233	1,233	1,233	1,233
Ray validation time (seconds)	596	657	836	1,427	2,843	6,203
Total time using this paper (seconds)	1,829	1,890	2,069	2,660	4,076	7,436
Reduction	-192.64%	-153.69%	-82.45%	-11.91%	24.82%	39.97%

edge diffraction with a maximum of 2 diffraction allowed in LOS and NLOS configurations respectively. The computation of visibility table for the receiver route takes 1,036 seconds and 1,502 seconds for LOS and NLOS scenario respectively. It can be seen that no reduction in ray validation is achieved for up to 2^{nd} order of rays computations. For 3^{rd} and 4^{th} order of ray interactions, the proposed model reduces the ray validation time by 25.95% and 43.54% respectively for LOS scenario and by 8.92% and 36.51% respectively for NLOS scenario. Given that vehicles move along fixed routes in an urban environment, the visibility information for all possible receiver locations can be pre-computed. This database can be used to create the visibility table for each receiver, essentially eliminating the computational cost documented in the second row of tables 2 to 5. This will further increase the computational gain of the proposed algorithm, and the maximum reduction obtainable in this case is given by the final row of table 5.

Table 6 compares the time reduction achieved for the computation of diffuse scattering rays using the proposed model against the space-division technique for both LOS and NLOS configurations. The space-division technique takes 78,039 seconds and 87,338 seconds for the computation of valid diffused scattering rays in LOS and NLOS scenario respectively. The proposed algorithm takes a total of 6,953 seconds and 6,185 seconds for the computation of diffused scattering rays in LOS and NLOS scenarios respectively. This corresponds to a time reduction of 91.09% and 92.92% for LOS and NLOS scenario respectively.

Table 4: Ray-tracing time comparison for combination of wall reflections and vertical edge diffraction in LOS scenario.

Time	Order = 1	Order = 2	Order = 3	Order = 4
Total time using [4] (seconds)	674	1,664	4,485	10,780
Pre-process time for RX route (seconds)	1,036	1,036	1,036	1,036
Ray validation time (seconds)	655	1,064	2,285	5,050
Total time using this paper (seconds)	1,691	2,100	3,321	6,086
Reduction	-150.89%	-26.20%	25.95%	43.54%

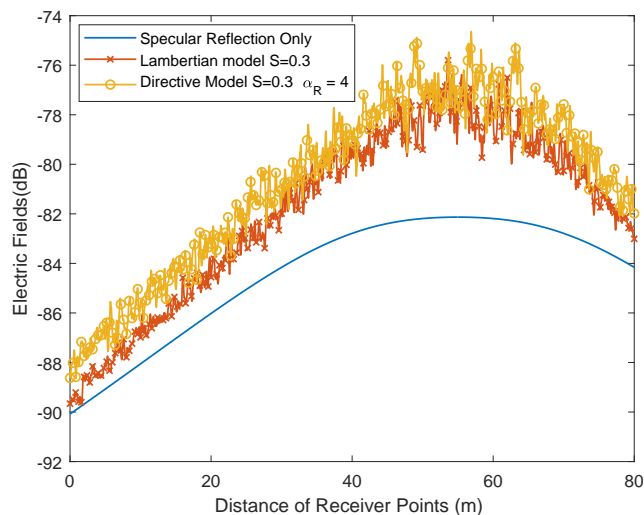


Figure 6: Comparison of specular reflection and specular reflection with diffuse scattering [8] for a test scenario in Fig. 5.

4 Conclusion

An efficient ray-tracing algorithm for vehicle-to-vehicle propagation modeling is presented in this paper. The proposed algorithm is based on the extension of previous model that makes use of the intra-visibility matrix to immediately produce image-tree for the mobile transmitter. The model pre-computes the receiver’s visibility table that contains the list of faces and edges directly visible to the mobile receiver. A one-on-one matching is performed to identify the common nodes in the transmitter’s image-tree and the receiver’s visibility table. The model expedites the ray-tracing as a smaller image-tree with viable nodes that can produce valid rays at the receiver need be checked. A time-efficient technique to identify the section on building facades commonly visible to both the transmitter and receiver that contributes diffuse scattering is also proposed using the intra-visibility matrix. The model performance is investigated by way of a comparison of the ray validation time required for vehicle-to-vehicle communication scenarios at an urban street intersection. The proposed model reduces the ray validation time by up to 47% for higher order of specular ray interaction and by up to 92% for diffuse scattering contributions which makes it a suitable candidate for propagation prediction in vehicular networks.

References

- [1] A. F. Molisch, F. Tufvesson, J. Karedal, and C. F. Mecklenbräuker, “A survey on vehicle-to-vehicle propagation channels,” *IEEE Wirel. Commun.*, vol. 16, no. 6, 2009.

Table 5: Ray-tracing time comparison for combination of wall reflections and vertical edge diffraction in NLOS scenario.

Time	Order = 1	Order = 2	Order = 3	Order = 4
Total time using [4] (seconds)	671	1,584	4,272	10,760
Pre-process time for <i>RX</i> route (seconds)	1,502	1,502	1,502	1,502
Ray validation time (seconds)	629	1,096	2,389	5,330
Total time using this paper (seconds)	2,131	2,598	3,891	6,832
Reduction	-217.59%	-64.20%	8.92%	36.51%
Reduction with pre-computed <i>RX</i> route visibility	6.26%	30.81%	44.08%	50.46%

Table 6: Ray-tracing time comparison for diffuse scattering in LOS and NLOS scenario.

Time	LOS Case	NLOS Case
Using space-division technique (seconds)	78,039	87,338
Pre-process time for <i>RX</i> route (seconds)	605	625
Diffuse scattering time using visibility matching (seconds)	6,348	5,560
Total time using this paper (seconds)	6,953	6,185
Reduction	91.09%	92.92%

- [2] D. Bilibashi, E. M. Vitucci and V. Degli-Esposti, "Dynamic ray tracing: introduction and concept," *14th Eur. Conf. Antennas Propagation*, EuCAP, 2020.
- [3] F. Quatresooz, S. Demey and C. P. Oestges, "Tracking of interaction points for improved dynamic ray tracing," *IEEE Trans. Veh. Technol.*, vol. 70, no. 7, 2021.
- [4] S. Hussain and C. Brennan, "Efficient pre-processed ray-tracing for 5G mobile transmitter scenarios in urban microcellular environments," *IEEE Trans. Antennas Propag.*, vol. 67, no. 5, 2019.
- [5] —, "A dynamic visibility algorithm for ray tracing in outdoor environments with moving transmitters and scatterers," *14th Eur. Conf. Antennas Propagation*, EuCAP 2020.
- [6] J. C. de Silva and E. Costa, "A ray-tracing model for millimeter-wave radio propagation in dense-scatter outdoor environments," *IEEE Trans. Antennas Propag.*, vol. 69, no. 12, 2021.
- [7] T. Abbas, J. Nuckelt, T. Kürner, T. Zemen, C. F. Mecklenbräuker and F. Tufveson, "Simulation and measurement-based vehicle-to-vehicle channel characterization: accuracy and constraint analysis," *IEEE Trans. Antennas Propag.*, vol. 63, no. 7, 2015.
- [8] V. Degli-espsti, F. Fuschini, E. M. Vitucci and G. Falciasacca, "Measurement and modelling of scattering from buildings," *IEEE Trans. Antennas Propag.*, vol. 55, no. 1, 2007.
- [9] N. Dreyer and T. Kurner, "An analytical ray-tracer for efficient D2D path loss predictions," *13th Eur. Conf. Antennas Propagation*, EuCAP, 2019.

- [10] "COST 231 Munich digital map and measurements". Accessed on: Nov. 10, 2020. [online]. Available: <https://propagationtools.com/wireless/cost-231-munich-digital-map-and-measurements/>
- [11] S. Hussain and C. Brennan, "An image visibility based pre-processing method for fast ray tracing in urban environments," in *10th Eur. Conf. Antennas Propagation*, EuCAP 2016.